Environmental Science and Pollution Research (2020) 27:40504–40511
https://doi.org/10.1007/s11356-020-10072-z

RESEARCH ARTICLE

Experimental and theoretical study of kinetic and mechanism of hydroxyl radical-mediated degradation of sulfamethazine

Xie Zheng[1,2] · Shijie Chen[1,2] · Lingwei Gao[3] · Yucheng Liu[1,2] · Fenghua Shen[1,2] · Hui Liu[1,2]

Received: 6 April 2020 / Accepted: 8 July 2020 / Published online: 14 July 2020

Abstract

Hydroxyl radical (•OH)-based advanced oxidation technologies (AOTs) is an effective and clean way to remove sulfonamide antibiotics in water at ambient temperature and pressure. In this study, we systematically investigated the degradation kinetics of sulfamethazine (SMT) by •OH with a combination of experimental and theoretical approaches. The second-order rate constant (k) of SMT with •OH was experimentally determined to be $5.27 \pm 0.06 \times 10^9$ M^{-1} s^{-1} at pH 4.5. We also calculated the thermodynamic and kinetic behaviors for the reactions by density functional theory (DFT) using the B3LYP/6-31G*. The results revealed that •OH addition pathways at the methylene (C4) site on the pyridine ring and the ortho sites (C12 and C14) of the amino group on the benzene ring dominate the reaction, especially C14 site on the benzene ring accounted for 43.95% of SMT degradation kinetics. The theoretical k value which was calculated by conventional transition state theory is 3.96×10^9 M^{-1} s^{-1}, indicating that experimental observation ($5.27 \pm 0.06 \times 10^9$) is correct. These results could further help AOTs design in treating sulfonamide during wastewater treatment processes.

Keywords Hydroxyl radical · Sulfamethazine · UV/H_2O_2 · Pathway · Kinetics · DFT

Introduction

Pharmaceutical such as analgesics, antibiotics, steroid, and hormones are widely used in the medical and health field nowadays. However, they are ineffective and low in biodegradability in the activated sludge process treatment method (Lapworth et al. 2012). For example, the total removal efficiencies (including sorption and biodegradation) of metronidazole, sulfamethoxazole, and carbamazepine in activated sludge process were only 61.7, 56.7, and 9.0% at 24 h, respectively (Min et al. 2018). Thus, these pharmaceuticals are observed frequently in secondary effluent of sewage treatment plant (Benitez et al. 2011; Wei et al. 2019). Sulfamethazine (SMT) is one of the best-seller broad-spectrum antibiotics with a structural analog of para-aminobenzoic acid (Luo et al. 2018b; Mao et al. 2019). Although the concentrations detected in aquatic environment are very low (from ng L^{-1} to μg L^{-1}) (Managaki et al. 2007; Jiang et al. 2011; Yan et al. 2013), SMT have long-term adverse effects on aquatic ecosystems and human health (Noguera-Oviedo and Aga 2016; Luo et al. 2018b; Gao et al. 2019), even causing microorganisms to develop antibiotic-resistant genes (Hsu et al. 2014). Therefore, an effective and environmental-friendly treatment technology to remove SMT and related antibiotics is urgently required.

Advanced oxidation technologies (AOTs) is an effective and clean way to remove antibiotics in water treatments. The hydroxyl radical (•OH) are the most important and widely

Responsible editor: Vítor Pais Vilar

Electronic supplementary material The online version of this article (https://doi.org/10.1007/s11356-020-10072-z) contains supplementary material, which is available to authorized users.

✉ Hui Liu
leolau@csu.edu.cn

[1] Institute of Environmental Engineering, School of Metallurgy and Environment, Central South University, Changsha 410083, China

[2] Chinese National Engineering Research Center for Control & Treatment of Heavy Metal Pollution, Changsha 410083, China

[3] School of Environment, Beijing Key Laboratory for Emerging Organic Contaminants Control, State Key Joint Laboratory of Environmental Simulation and Pollution Control, Tsinghua University, Beijing 100084, China

applied free radicals in AOTs, which generates at normal experimental conditions with highly reactive and high redox potential (Ghernaout 2013; Xiao et al. 2017; Mao et al. 2019). Although there are some studies for the removal efficiency and degradation kinetic of SMT in Fenton-like (Pérez-Moya et al. 2010; Zhou et al. 2013; Pan et al. 2018), the mechanistic aspects of SMT degradation by $^{\bullet}OH$ still remain unclear. Due to the limitation of experimental techniques, theoretical research can provide compelling evidence of degradation mechanistic.

The density functional theory (DFT) is one of the most powerful tools to provide deeper sights in reaction kinetics, reaction mechanisms, which has been successfully applied to investigate AOTs' oxidation of organic pollutants (Qu et al. 2016; Zeng et al. 2016; Zhao et al. 2016; Luo et al. 2017a, b; Xiao et al. 2017). Unfortunately, only a few DFT studies can be found on the radical-mediated degradation mechanisms of SMT in AOTs. Yin investigated the degradation pathway and mechanism of SMT oxidation by $SO_4^{\bullet-}$ at the B3LYP/6–31 + G** level of theory. The calculation results showed $SO_4^{\bullet-}$ are more likely to attack the S–N, S–C, and N–C bonds and addition on the benzene ring (Yin et al. 2018). However, different from $SO_4^{\bullet-}$ oxidation of SMT, there are intrinsic differences between $^{\bullet}OH$ and SMT yield different reaction pathways (i.e., single electron transfer (SET), hydrogen atom transfer (HAT), and radical adduct formation (RAF)) and they show different reactivities. There is lack of literature combination of experimental and DFT method for $^{\bullet}OH$-mediated degradation of SMT.

In this study, we investigated the thermodynamics and kinetics of SMT degradation in UV/H_2O_2 system by combining experimental and theoretical approaches. The experiment was conducted using the competition kinetics method to measure k value of SMT reacting with $^{\bullet}OH$. The DFT calculation was used to investigate the reaction pathways, kinetics, and mechanisms of SMT with $^{\bullet}OH$. Then the different pathway's contribution to overall degradation was revealed. This study intended to elucidate the mechanisms of $^{\bullet}OH$ oxidation of SMT in molecular level and promoted further practically of AOTs for treatment of antibiotics.

Materials and methods

Materials

Sulfamethazine (SMT, > 99%), H_3PO_4 (85–90%), Na_2HPO_4 (99%), NaH_2PO_4 (99%), and acetophenone (ACP, > 99%) were purchased from Sigma-Aldrich and used without further purification. H_2O_2 (30% by weight), H_2SO_4 (guaranteed reagent), $KMnO_4$ (analytical grade), and $Na_2C_2O_4$ (analytical grade) were purchased from Sinopharm Chemical Reagent, China. H_3PO_4, Na_2HPO_4, and NaH_2PO_4 were used as buffer system. H_2O_2 was used as precursor to generate $^{\bullet}OH$ under UV irradiation. H_2SO_4, $KMnO_4$, and $Na_2C_2O_4$ were used for average light intensity per volume (I_0) and optical path (l) measurements. ACP was chosen as a reference compound to determine the k value of $^{\bullet}OH$ oxidation of SMT. All solutions were prepared using deionized (DI) water from a molecular water system (Molresearch 1010A). The S220 pH meter (Mettler Toledo) is used to measure solution pH.

Photochemical experiments

The photochemical reactor used in this study has been described in detail in our previous work. (Luo et al. 2018a). A 10 W low-pressure UV lamp (GPH212T5L/4, Heraeus) was used as the light source to activate H_2O_2-producing $^{\bullet}OH$, which was placed in the center of quartz trap in 50-mL photochemical reactor. A water-cooling system (SC150 − A25B, Thermo Fisher Scientific) was used to maintain the temperature of reactor solution at 20 ± 1 °C. The Teflon magnetic bars were used to stir the reaction solution. The initial concentration ratio of SMT (10 μM) to H_2O_2 (100 μM) was 1:10 in order to ensure that H_2O_2 was excessive. The initial concentration of ACP was consistent with SMT. The phosphate buffer (10 mM) composed of H_3PO_4, NaH_2PO_4, and Na_2HPO_4 was used to keep solution at pH = 4.5, to ensure the majority species of SMT was on its neutral form during the experiment. The ratio of neutral form was 99.9% obtained from its acid dissociation constant ($pK_{a1} = 2.26$, $pK_{a2} = 7.65$) of SMT (Benitez et al. 2011; Lin et al. 1997a, b). A 2.5-mL glass syringe (Gastight 1001, Hamilton) was used to take 0.6-mL sample from the reactor at the designed time.

In order to determine second-order rate constant (k) of SMT reacting with $^{\bullet}OH$, ACP was used as a reference compound for the competition kinetics method in the $^{\bullet}OH$-mediated oxidation system (Packer et al. 2003). First, ACP was not dissociated at all pH and remains at neutral form. Second, the k values of ACP ($k = 5.9 \times 10^9\ M^{-1}\ s^{-1}$) were at the same order of magnitude with most organic contaminant that react with $^{\bullet}OH$, which can ensure similar competitive ability to $^{\bullet}OH$ (Xiao et al. 2017). Therefore, Eq. (1) was used to calculate the k_{SMT} value in our system.

$$\frac{k_{SMT}}{k_{ACP}} = \frac{\ln\frac{[SMT]_t}{[SMT]_0}}{\ln\frac{[ACP]_t}{[ACP]_0}} = \frac{\left(\ln\frac{[SMT]_t}{[SMT]_0}\right)_{UV}}{\left(\ln\frac{[ACP]_t}{[ACP]_0}\right)_{UV}} = \frac{\ln\frac{[SMT]_t}{[SMT]_0} - k'_{SMT,UV}}{\ln\frac{[ACP]_t}{[ACP]_0} - k'_{ACP,UV}} \quad (1)$$

where $k'_{SMT,UV}$ and $k'_{ACP,UV}$ are the apparent rate constants for the direct photolysis of SMT and ACP by ultraviolet, respectively. All the experiments were carried out in triplicate.

Analytical and computational methods

The ultra-performance liquid chromatography (UPLC, Waters ACQUITY H–Class, BEH C18 column, 1.7 μm, 50 × 2.1 mm) with PDA detector (UV) was used to quantify SMT and ACP. The column temperature was kept at 35 °C, and the mobile phase was composed of 20% acetonitrile and 80% phosphoric buffer (20 mM at pH 3) with a flow rate of 0.3 mL min^{-1}. The wavelengths of UV detector were set at 238 nm and 255 nm, respectively, to determine concentrations of SMT and ACP. A UV–1800 spectrometer (Shimadzu, Japan) was used to determine the maximum absorption of SMT from 200 to 400 nm.

The thermodynamics and kinetics for the reaction of SMT and ·OH were studied using Gaussian 09 program package (Revision A.01) with DFT approach based on B3LYP/6–31 + G** level of theory. The second-order rate constant (k) of SMT reacting with ·OH was calculated using the convention transition state theory (TST). The detailed computational methods were shown on Text A1, SI. The distribution of highest occupied molecular orbital (HOMO) and lowest unoccupied molecular orbital (LUMO) were used to characterize the electron density distribution of molecules.

Results and discussion

Direct UV photolysis of sulfamethazine

The direct UV photolysis of sulfamethazine was calculated by Beer-Lambert law. The detailed calculation process was shown at Text A2, SI. The initial direct photolysis degradation rate (r_{UV}) of sulfamethazine was determined to be (3.00 ± 0.21) × 10^{-7} M min^{-1} at $[SMT]_0$ = 10 μM. The average light intensity per volume (I_0) was determined to 1.89 × 10^{-6} Einstein L^{-1} s^{-1}, and the effective optical pathlength (l) was 1.41 cm determined by H_2O_2 actinometry method. The molar absorption coefficient (ε, M^{-1} cm^{-1}) value of SMT was determined to be 18,460 M^{-1} cm^{-1} at 254 nm in this study (Fig. A1, SI), which was consistent with the reported values; 16,196 M^{-1} cm^{-1} at pH = 3.6; and 18,525 M^{-1} cm^{-1} at pH = 7.85 (Baeza and Knappe 2011). The quantum yield (φ, mol $Einstein^{-1}$) of SMT was determined to be (7.90 ± 0.21) × 10^{-3} mol $Einstein^{-1}$ at 254 nm.

OH-mediated degradation of sulfamethazine

We analyzed the concentration variations of SMT in the dark control within 24 h. The result showed that the SMT concentration has not changed at all during the experiment, which illustrated that there was no reaction between SMT and H_2O_2. The SMT degradation in UV/H_2O_2 systems usually consists of two parts: the direct photolysis and ·OH oxidation. Therefore, the first-order rate constant k' (min^{-1}) of SMT in our system can be calculated as

$$-\frac{dC}{dt} = k'C = \left(k'_{UV} + k'_{\cdot OH}\right)C \quad (2)$$

where the k'_{UV} and $k'_{\cdot OH}$ are the apparent rate constants in UV and UV/H_2O_2 system, respectively.

As shown in Fig. 1 ($R^2 > 0.95$), the degradation kinetics of SMT agreed with the pseudo first-order kinetics model. The apparent degradation rate constant of SMT in the UV system was 0.030 min^{-1}. The degradation kinetics processes of SMT were enhanced due to the addition of H_2O_2 (100 μM) (Fig. 1). The apparent rate constant of SMT in the UV/H_2O_2 system was 0.045 min^{-1}, which is 1.5 times larger than that in the UV system. The UV can active the H_2O_2 to produce the oxidizing ·OH. The enhanced degradation of SMT after the addition of H_2O_2 was attributed to ·OH-mediated oxidation reaction (33.3%). The k value of SMT reacting with ·OH was determined to be (5.27 ± 0.06) × 10^9 M^{-1} s^{-1}, which was consistent with the reported value from literatures (Table A1, SI).

Theoretical thermodynamics and kinetics

Three reaction pathways (i.e., single electron transfer (SET), hydrogen atom transfer (HAT), and radical adduct formation (RAF)) for the first step of ·OH oxidation of SMT were calculated based on DFT method. The optimized SMT molecule and the degradation pathway are shown in Fig. A2, SI and Fig. 2, respectively. The calculated thermodynamics and

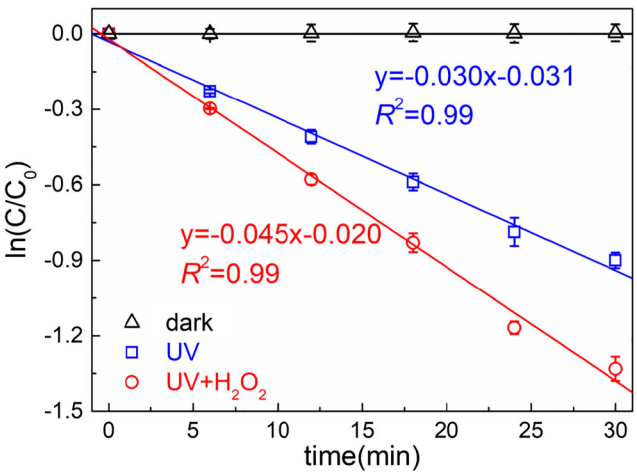

Fig. 1 Time-dependent degradation kinetics of SMT in the dark, UV, and UV/H_2O_2 system ($[SMT]$ = 10 μM, $[H_2O_2]$ = 100 μM, pH = 4.5 and I_0 = 1.89 × 10^{-6} Einstein L^{-1} s^{-1}). The degradation was fitted to a first-order kinetic model (lines)

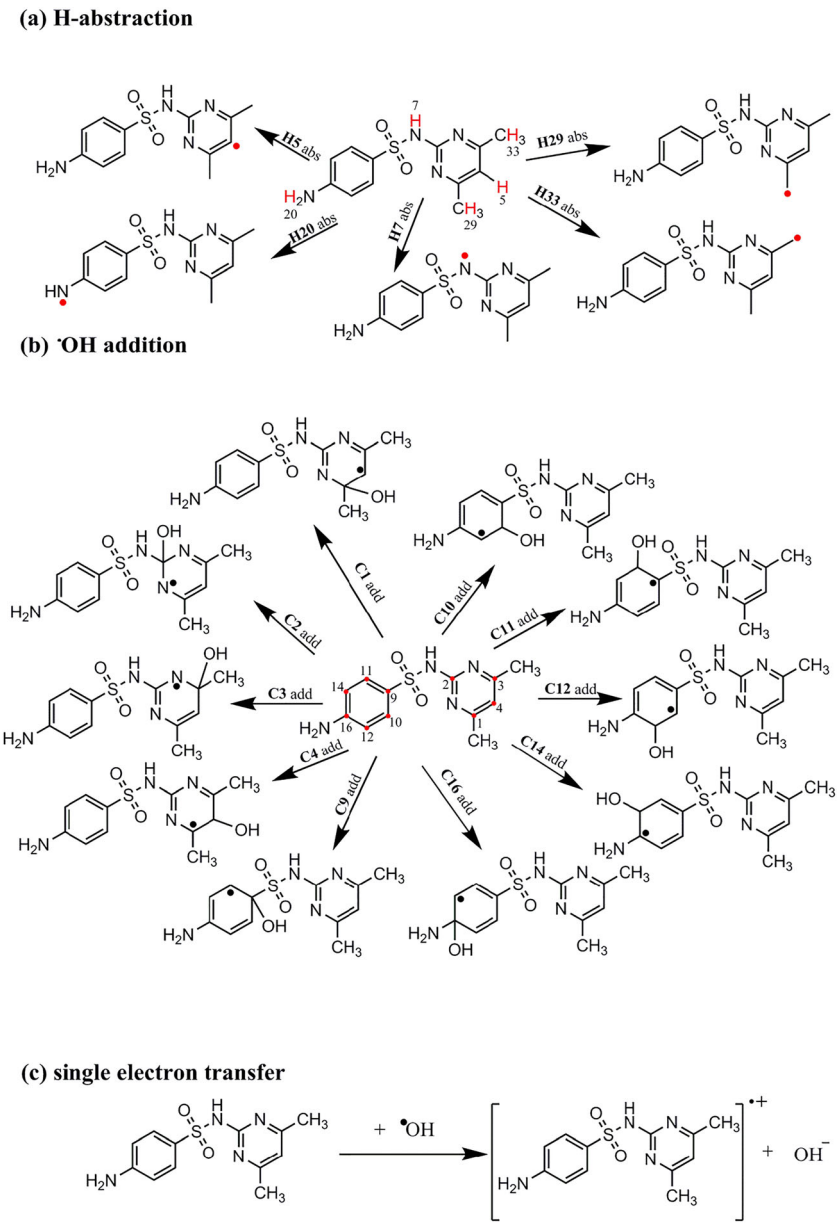

Fig. 2 The selected pathways for the reactions of neutral SMT with ·OH based on (**a**) H abstraction, (**b**) ·OH addition, and (c) SET

kinetics parameters for the reaction of SMT with ·OH are tabulated in Table 1.

For the SET pathway, as shown in Table 1, the reaction is thermodynamically unfavorable with ΔG_R° = 17.29 kcal mol^{-1}. It is expected, due to SMT molecule containing the –CH_3, –NH_2, and –SO_2 − NH− groups were weak and strong in electron-donating abilities, and strong electron-withdrawing group, respectively. Many studies indicated that for the SET pathway of ·OH-mediated oxidation of organic compounds, only strong electron-donating groups are thermodynamically favorable (Luo et al. 2017a, b, 2018a). The weak electron-donating and strong electron-withdrawing groups reduce the likelihood of SET reaction. For the HAT pathways, the values of ΔH_R° were between −27.37 and −3.25 kcal mol^{-1}, and the values of ΔG_R° were between −27.72 and −4.69 kcal mol^{-1} (Table 1), which indicated that ·OH can abstract the H atom from group = CH− (H5), −NH −(H7), −NH_2 (H20), –CH_3 (H29, H33). The values of $\Delta^\ddagger G^\circ$ of HAT were between 6.72 and 10.76 kcal mol^{-1}. For ·OH addition pathways, all of the reactions are thermodynamically favorable processes (ΔG_R° <0) except for the addition process on C1 (ΔG_R° = 1.06 k cal mol^{-1}), C2 (ΔG_R° = 0.23 kcal mol^{-1}), and C16 (ΔG_R° = 0.23 kcal mol^{-1}). The values of ΔH_R° via ·OH addition were between −51.60 and −0.04 kcal mol^{-1} and the values of $\Delta^\ddagger G^\circ$ were between 4.50 and 17.27 kcal mol^{-1} expect for the addition process on C1, C2, and C16 (Fig. 3).

Table 1 Activation energy $\Delta^{\ddagger}G^{\circ}$(kcal mol^{-1}), Gibbs free to change ΔG_R° (kcal mol^{-1}), enthalpy change ΔH_R° (kcal mol^{-1}), imaginary frequencies (cm^{-1}), and second-order rate constants k (M^{-1} s^{-1}) for the transition state species involved in the reactions of SMT with •OH calculated at IEFPCM/B3LYP/6–311++G**//B3LYP/6–31 + G** level of theory

Reaction pathway	Position	ΔH_R°	ΔG_R°	$\Delta^{\ddagger}G^{\circ}$	Imaginary frequency	k_1	θ
•OH addition	C1	−8.96	1.06	12.83	−381	1.84×10^3	0.00%
	C2	−10.48	0.23	17.27	−555	1.18×10^0	0.00%
	C3	−9.74	−0.04	12.51	−364	3.13×10^3	0.00%
	C4	−13.21	−4.46	4.89	−164	9.82×10^8	24.81%
	C9	−57.59	−51.60	7.54	−121	1.25×10^7	0.31%
	C10	−11.86	−1.50	10.26	−431	1.48×10^5	0.00%
	C11	−11.33	−1.35	11.06	−420	3.78×10^4	0.00%
	C12	−14.25	−4.53	4.90	−190	9.66×10^8	24.42%
	C14	−14.73	−5.50	4.50	−181	1.74×10^9	43.95%
	C16	−9.30	0.23	9.86	−382	2.79×10^5	0.01%
H abstraction	H5	−3.25	−4.69	10.76	−1322	1.43×10^5	0.00%
	H7	−19.97	−21.79	6.72	−1313	1.29×10^8	3.25%
	H20	−24.00	−24.87	8.08	−460	1.19×10^7	0.30%
	H29	−27.17	−27.40	7.10	−341	8.57×10^7	2.16%
	H33	−27.37	−27.72	7.72	−382	3.10×10^7	0.78%
SET		22.99	17.29	23.18			
					overall	3.96×10^9	100%

It should be noted that the $\Delta^{\ddagger}G^{\circ}\Delta^{\ddagger}G^{\circ}$ of •OH addition reaction on C4, C12, and C14 site is obviously lower than other reaction pathways. That is attributed to the different electron-donating and electron-withdrawing abilities of different groups. The $-CH_3$ and $-NH_2$ are weak and moderate electron-donor group, respectively, which increase the electron density of the C4, C12, and C14 sites. Further, the electron density of C12 and C14 sites are higher than C4 due to the electron-donating abilities of $-NH_2$ are higher than $-CH_3$. However, sulfur-containing groups ($-SO_2-NH-$) are a strong electron-withdrawing group that would decrease the electron density of C2, C9, C10, and C11 sites. Thus, the reactivity of •OH with C2, C9, C10, and C11 sites is decreased. As shown in Table 1, the RAF reaction of C4, C12, and C14 site accounts for 93.18% (θ) of •OH–mediated SMT degradation kinetics, indicating three primary reaction channels.

The second-order rate constant (M^{-1} s^{-1}) between SMT and •OH was calculated by using conventional TST. In addition, the Wigner's approach was used to correct tunneling of every reaction channel. The calculated k values for H abstractions range from 1.43×10^5 to 1.29×10^8 M^{-1} s^{-1} (average 5.15×10^7 M^{-1} s^{-1}). For •OH addition pathways, the k values range from 1.18×10^0 to 1.74×10^9 M^{-1} s^{-1} (average 3.70×10^8 M^{-1} s^{-1}). It should be noted that the average k value of •OH addition pathways is 7.19 times than that of H abstraction pathways. The results stated that, in •OH oxidation of SMT, the H abstraction pathways were almost negligible and the •OH addition pathways in C4, C12, and C14 sites were the dominate reaction, especially C14 site accounted for 43.95%

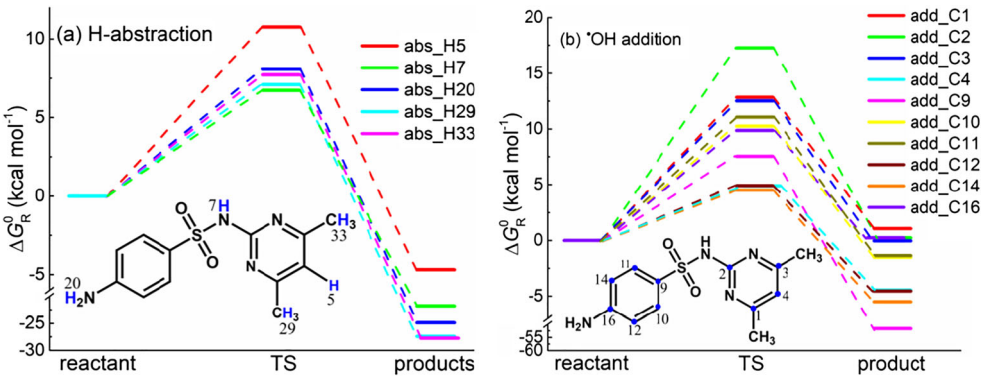

Fig. 3 The potential energy surface for the reaction between SMT and •OH at IEFPCM/B3LYP/6–311++G**//B3LYP/6–31 + G** level of theory

of SMT degradation kinetics. The overall theoretical k value was calculated to be 3.96×10^9 M^{-1} s^{-1}, which showed a good agreement with the experimental k value (5.27×10^9 M^{-1} s^{-1}) in this paper. The Γ values of $^{\bullet}OH$ addition pathways were not large (from 1.01 to 1.30) for their low barriers. However, for H abstraction pathway, the Γ values were from 1.11 to 2.70, because of their high activation energy barriers (6.72 to 10.76 kcal mol^{-1}), which were obviously higher than $^{\bullet}OH$ addition pathways.

Mechanistic interpretation for SMT degradation

According to the literatures, several intermediates were reported in sulfonamides degradation under different conditions (Boreen et al. 2004; García-Galán et al. 2008; Trovó et al. 2009; Rodayan et al. 2010; Gao et al. 2012; Guo et al. 2012), amd some relevant products were shown in Table 2. The dark control results showed that there is no reaction between SMT and H_2O_2. Therefore, the degradation of SMT during UV/H_2O_2 was mainly due to the oxidation by $^{\bullet}OH$ radical.

Table 2 The observed reaction intermediates from the reaction of $^{\bullet}OH$ and SMT

#	structure	molecular formula	molecular weight (g mol^{-1})	Ref.
P1	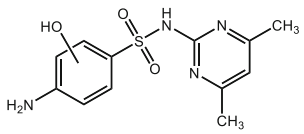	$C_{12}H_{14}N_4O_3S$	294	(Gao and Gao et al., 2012; Yin and Guo et al., 2018)
P2	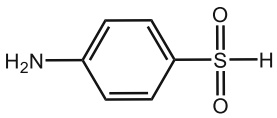	$C_6H_7NO_2S$	157	(Yin and Guo et al., 2018)
P3	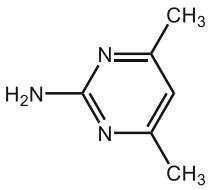	$C_6H_9N_3$	123	(Liu and Wang, 2013; Yin and Guo et al., 2018)
P4	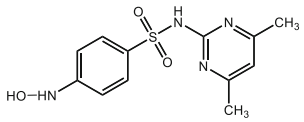	$C_{12}H_{14}N_4O_3S$	294	(Yin and Guo et al., 2018)
P5	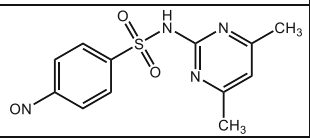	$C_{12}H_{12}N_4O_3S$	292	(Yin and Guo et al., 2018)
P6	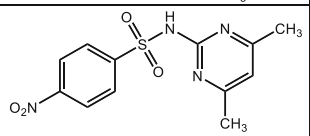	$C_{12}H_{12}N_4O_4S$	308	(Yin and Guo et al., 2018)
P7	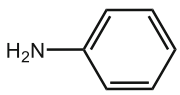	C_6H_7N	93	(Liu and Wang, 2013; Yin and Guo et al., 2018)
P8	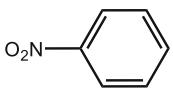	$C_6H_5NO_2$	123	(Yin and Guo et al., 2018)

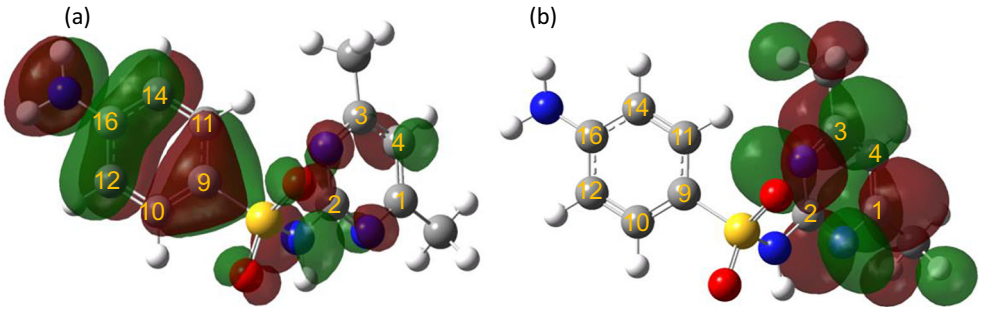

Fig. 4 The HOMO and LUMO distribution of SMT (a) & (b) calculated at B3LYP/6–31 + G** theory level. The red and green colors represent the positive and negative phases of the molecular orbitals

The SET reactions thermodynamically were unfavorable due to the presence of weak electron-donating group (–CH_3), which reduced the likelihood of SET reaction. The $^{\bullet}$OH was able to abstract an H atom from = CH−, −NH−, $-NH_2$, $-CH_3$ groups to form H_2O and SMT radical (SMT$^{\bullet}$). However, it was an unfavorable high-energy process to occur H-abstraction on $-CH_3$ site and form an unstable methyl radical ($-CH_3^{\bullet}$) (Luo et al. 2018a). Loss of H20 from the $-NH_2$ group results in the formation of stable amino radical (−NH$^{\bullet}$) which is vulnerable to attack by extra $^{\bullet}$OH and then form the reaction product P4 (Table 2) by radical coupling reaction. The $^{\bullet}$OH oxidation of P4 leads to P5 and P6. The C-S and N-S bond concentrated at the center of SMT molecule, which were easily destroyed due to the attacks by $^{\bullet}$OH. The $^{\bullet}$OH can easily attacked the N−H bond (H7) because the nitrogen atom was strong negative charge, leading to generate an unstable SMT radical. The N-S bond in SMT radical breaks rapidly, which leads to the formation of P2 and P3. P2 can undergo a series of reactions such as desulfation and oxidation reaction and then generate P7 and P8.

The HOMO and LUMO distributions well clarified the mechanism of $^{\bullet}$OH addition on SMT molecule, which reflected the π bonding orbital and anti-bonding π* orbital, respectively (Yang et al. 2017; Luo et al. 2018a). As expected, Fig. 4 showed that the HOMO distributed in the benzene ring and C4 site; meanwhile the LUMO distributed in the pyrimidine ring. The frontline molecular orbit suggested that $^{\bullet}$OH was more likely to attack these electron rich regions. Therefore, the $^{\bullet}$OH was more likely to adduct at C4, C12, and C14 sites, and their $\Delta^{\ddagger}G^{\circ}$ values were 4.89, 4.90, and 4.50 kcal mol^{-1}, respectively. The $^{\bullet}$OH addition at C14 was the preferred reaction due to the electron-donor group $-NH_2$ increased the electron density on its ortho sites (C14). Meanwhile the C9 and C12 sites showed less reactivity because of the presence of electron-withdrawing group $-SO_2-$ NH−.

Conclusion

The degradation processes of SMT in the UV/H_2O_2 system was studied by combining experimental and theoretical approach. The results showed the degradation kinetics of SMT was significantly enhanced in UV system after the addition of H_2O_2. It was attributed to $^{\bullet}$OH-mediated oxidation. The k value determined by competitive kinetics was $(5.27 \pm 0.06) \times 10^9$ M^{-1} s^{-1}, which is consistent with experimental value and reported values by previous. The three degradation pathways of SMT were calculated at the IEFPCM/B3LYP/6–311++G**//B3LYP/6–31 + G** level of theory. The calculated results indicated that the RAF pathways are more favorable than HAT pathways and $^{\bullet}$OH addition into C4, C12, and C14 site dominates the reaction, especially C14 site which is accounted for 43.95% of SMT degradation kinetics. Moreover, the energy barriers, electron donor/withdraw abilities of group, and HOMO and LUMO distribution were studied to reveal the reaction mechanism. It should be noted that the degradation yielded several sub-products with uncertain toxicity, such as aromatic amines may be more carcinogenic, mutagenic, and genotoxic than SMT. Nonetheless, the degradation pathways are significant, the mechanism of $^{\bullet}$OH oxidation SMT based on experimental and theoretical calculation can help further evaluate the removal efficiency and extend the application in AOTs' degradation of sulfonamide antibiotics during wastewater treatment processes.

Acknowledgments Funding from National Nature Science Foundation of China (21806035) and National Nature Science Foundation of Hunan province (2019JJ50226). The key projects of Science and Technology of Hunan Province (2017SK2420) are gratefully acknowledged.

References

Baeza C, Knappe DRU (2011) Transformation kinetics of biochemically active compounds in low-pressure UV photolysis and UV/H2O2 advanced oxidation processes. Water Res 45(15):4531–4543

Benitez FJ, Acero JL, Real FJ, Roldan G, Casas F (2011) Comparison of different chemical oxidation treatments for the removal of selected pharmaceuticals in water matrices. Chem Eng J 168(3):1149–1156

Boreen AL, Arnold WA, McNeill K (2004) Photochemical fate of sulfa drugs in the aquatic environment: sulfa drugs containing five-

membered heterocyclic groups. Environ Sci Technol 38(14):3933–3940

Gao Y, Gao N, Deng Y, Yang YQ, Ma Y (2012) Ultraviolet (UV) light-activated persulfate oxidation of sulfamethazine in water. Chem Eng J 195-196:248–253

Gao L, Minakata D, Wei Z, Spinney R, Dionysiou DD, Tang CJ, Chai L, Xiao R (2019) Mechanistic study on the role of soluble microbial products in sulfate radical-mediated degradation of pharmaceuticals. Environ Sci Technol 53(1):342–353

García-Galán MJ, Silvia Díaz-Cruz M, Barceló D (2008) Identification and determination of metabolites and degradation products of sulfonamide antibiotics. TrAC Trends Anal Chem 27(11):1008–1022

Ghernaout D (2013) Advanced oxidation phenomena in electrocoagulation process: a myth or a reality? Desalin Water Treat 51(40–42):7536–7554

Guo Z, Zhou F, Zhao Y, Zhang C, Liu F, Bao C, Lin M (2012) Gamma irradiation-induced sulfadiazine degradation and its removal mechanisms. Chem Eng J 191:256–262

Hsu J, Chen C et al (2014) Prevalence of sulfonamide-resistant bacteria, resistance genes and integron-associated horizontal gene transfer in natural water bodies and soils adjacent to a swine feedlot in northern Taiwan. J Hazard Mater 277:34–43

Jiang L, Hu X et al (2011) Occurrence, distribution and seasonal variation of antibiotics in the Huangpu River, Shanghai, China. Chemosphere 82(6):822–828

Lapworth DJ, Baran N, Stuart ME, Ward RS (2012) Emerging organic contaminants in groundwater: a review of sources, fate and occurrence. Environ Pollut 163:287–303

Lin C, Chang C et al (1997a) Migration behavior and separation of sulfonamides in capillary zone electrophoresis II. Positively charged species at low pH. J Chromatogr A 759(1):203–209

Lin C, Lin W et al (1997b) Migration behavior and selectivity of sulfonamides in capillary electrophoresis. J Chromatogr A 792(1):37–47

Liu Y, Wang J, (2013) Degradation of sulfamethazine by gamma irradiation in the presence of hydrogen peroxide. J Hazard Mater (250–251):99–105

Luo S, Wei Z, Dionysiou DD, Spinney R, Hu WP, Chai L, Yang Z, Ye T, Xiao R (2017a) Mechanistic insight into reactivity of sulfate radical with aromatic contaminants through single-electron transfer pathway. Chem Eng J 327:1056–1065

Luo S, Wei Z, Dionysiou DD, Spinney R, Hu WP, Chai L, Yang Z, Ye T, Xiao R (2017b) Mechanistic insight into reactivity of sulfate radical with aromatic contaminants through single-electron transfer pathway. Chem Eng J 327:1056–1065

Luo S, Gao L, Wei Z, Spinney R, Dionysiou DD, Hu WP, Chai L, Xiao R (2018a) Kinetic and mechanistic aspects of hydroxyl radical–mediated degradation of naproxen and reaction intermediates. Water Res 137:233–241

Luo S, Wei Z, Spinney R, Villamena FA, Dionysiou DD, Chen D, Tang CJ, Chai L, Xiao R (2018b) Quantitative structure–activity relationships for reactivities of sulfate and hydroxyl radicals with aromatic contaminants through single–electron transfer pathway. J Hazard Mater 344:1165–1173

Managaki S, Murata A et al (2007) Distribution of macrolides, sulfonamides, and trimethoprim in tropical waters: ubiquitous occurrence of veterinary antibiotics in the mekong delta. Environmental Science & Technology 41(23):8004–8010

Mao Q, Zhou Y, Yang Y, Zhang J, Liang L, Wang H, Luo S, Luo L, Jeyakumar P, Ok YS, Rizwan M (2019) Experimental and theoretical aspects of biochar-supported nanoscale zero-valent iron activating H2O2 for ciprofloxacin removal from aqueous solution. J Hazard Mater 380:120848

Min X, Li W, Wei Z, Spinney R, Dionysiou DD, Seo Y, Tang CJ, Li Q, Xiao R (2018) Sorption and biodegradation of pharmaceuticals in aerobic activated sludge system: a combined experimental and theoretical mechanistic study. Chem Eng J 342:211–219

Noguera-Oviedo K, Aga DS (2016) Lessons learned from more than two decades of research on emerging contaminants in the environment. J Hazard Mater 316:242–251

Packer JL, Werner JJ, Latch DE, McNeill K, Arnold WA (2003) Photochemical fate of pharmaceuticals in the environment: naproxen, diclofenac, clofibric acid, and ibuprofen. Aquat Sci 65(4):342–351

Pan Y, Zhang Y, Zhou M, Cai J, Li X, Tian Y (2018) Synergistic degradation of antibiotic sulfamethazine by novel pre-magnetized Fe0/PS process enhanced by ultrasound. Chem Eng J 354:777–789

Pérez-Moya M, Graells M, Castells G, Amigó J, Ortega E, Buhigas G, Pérez LM, Mansilla HD (2010) Characterization of the degradation performance of the sulfamethazine antibiotic by photo-Fenton process. Water Res 44(8):2533–2540

Qu R, Liu J, Li C, Wang L, Wang Z, Wu J (2016) Experimental and theoretical insights into the photochemical decomposition of environmentally persistent perfluorocarboxylic acids. Water Res 104:34–43

Rodayan A, Roy R, Yargeau V (2010) Oxidation products of sulfamethoxazole in ozonated secondary effluent. J Hazard Mater 177(1):237–243

Trovó AG, Nogueira RFP, Agüera A, Sirtori C, Fernández-Alba AR (2009) Photodegradation of sulfamethoxazole in various aqueous media: persistence, toxicity and photoproducts assessment. Chemosphere 77(10):1292–1298

Wei Z, Li W, Zhao D, Seo Y, Spinney R, Dionysiou DD, Wang Y, Zeng W, Xiao R (2019) Electrophilicity index as a critical indicator for the biodegradation of the pharmaceuticals in aerobic activated sludge processes. Water Res 160:10–17

Xiao R, Gao L, Wei Z, Spinney R, Luo S, Wang D, Dionysiou DD, Tang C–J, Yang W (2017) Mechanistic insight into degradation of endocrine disrupting chemical by hydroxyl radical: an experimental and theoretical approach. Environ Pollut 231:1446–1452

Yan C, Yang Y, Zhou J, Liu M, Nie M, Shi H, Gu L et al (2013) Antibiotics in the surface water of the Yangtze Estuary: occurrence, distribution and risk assessment. Environ Pollut 175:22–29

Yang Z, Su R, Luo S, Spinney R, Cai M, Xiao R, Wei Z (2017) Comparison of the reactivity of ibuprofen with sulfate and hydroxyl radicals: an experimental and theoretical study. Sci Total Environ 590-591:751–760

Yin R, Guo W, Wang H, du J, Zhou X, Wu Q, Zheng H, Chang J, Ren N (2018) Enhanced peroxymonosulfate activation for sulfamethazine degradation by ultrasound irradiation: performances and mechanisms. Chem Eng J 335:145–153

Zeng X, Qu R, Feng M, Chen J, Wang L, Wang Z (2016) Photodegradation of Polyfluorinated Dibenzo-p-dioxins in organic solvents: experimental and theoretical studies. Environ Sci Technol 50(15):8128–8134

Zhao N, Zhang Q, Wang W (2016) Atmospheric oxidation of phenanthrene initiated by OH radicals in the presence of O2 and NOx—a theoretical study. Sci Total Environ 563-564:1008–1015

Zhou T, Wu X, Zhang Y, Li J, Lim TT (2013) Synergistic catalytic degradation of antibiotic sulfamethazine in a heterogeneous sonophotolytic goethite/oxalate Fenton-like system. Appl Catal B Environ 136-137:294–301